=== **CATALYTIC REACTION MECHANISMS** ===

Oxygen States in Oxides with a Perovskite Structure and Their Catalytic Activity in Complete Oxidation Reactions: System $La_{1-x}Ca_xFeO_{3-y}$ (x = 0–1)

L. A. Isupova, I. S. Yakovleva, V. A. Rogov, G. M. Alikina, and V. A. Sadykov

Boreskov Institute of Catalysis, Siberian Division, Russian Academy of Sciences, Novosibirsk, 630090 Russia
Received March 6, 2003

Abstract—Oxygen states in the $La_{1-x}Ca_xFeO_{3-y}$ perovskites prepared using different procedures are studied by temperature-programmed reduction (TPR). Results are compared to data on the catalytic activity in the oxidation of methane and carbon monoxide. The activity of the samples in the CO and CH_4 oxidation over a wide temperature range (200–600°C) is shown to correlate with the amount of reactive surface and subsurface oxygen removable during TPR below 420°C. These oxygen states in the samples of the $La_{1-x}Ca_xFeO_{3-y}$ series can be associated with the domain or intergrain boundaries. No correlation is found between the amount of lattice oxygen removable during TPR and the activity of the $La_{1-x}Ca_xFeO_{3-y}$ samples in the complete oxidation of methane at temperatures of 450–600°C. It is suggested that catalytic complete oxidation is determined by the most reactive surface and subsurface oxygen states located at the interphase boundaries, whereas the lattice oxygen does not participate in these reactions.

INTRODUCTION

Oxides with a perovskite structure, ABO_3, attract attention due to their high activity and stable performance in various oxidation reactions. The activity of perovskites in complete oxidation is known to be determined by the nature of a transition metal in the B-sublattice, its electron state depends on the substituting cations in the A and B sublattices, and the preparation conditions, which govern the real structure (microstructure) of the oxide [1–4]. The above factors determine the strength of the metal–oxygen bond on the oxide surface and consequently the complete oxidation rate [5, 6].

As was shown in [7], various oxygen states are present on the oxide surface, but only the most weakly bound ones, which are formed at extended defects on the surface, participate in complete oxidation. The participation of strongly bound lattice oxygen in complete oxidation is commonly excluded from consideration in these systems [6].

Oxygen states with different bonding strengths may be present on the perovskite surface, including weakly bound oxygen (for example, oxygen adsorbed on vacancies). However, the participation of the lattice oxygen in complete oxidation over the perovskite oxides has been discussed in the literature [8].

One of the most interesting systems in which the preparation procedure strongly affects the charge state of the transition metal, microstructure, and, hence, bond strength of the surface oxygen and the catalytic activity is the $La_{1-x}Ca_xFeO_{3-y}$ system, which is the subject of our study. When calcium is introduced into the system, depending on the preparation conditions, the

electroneutrality of the system is achieved either via the formation of oxygen vacancies and vacancy-ordered phases or by the formation of Fe^{4+} cations. For instance, in the system prepared by the "ceramic" procedure, the formation of three vacancy-ordered phases, which belong to the homologous series $A_nB_nO_{3n-1}$ (A = La, Ca; B = Fe), was found by Mössbauer spectroscopy and high-resolution electron microscopy: lanthanum ferrite with the perovskite structure, $LaFeO_3$ ($n = \infty$); calcium ferrite with the structure of brownmillerite, $Ca_2Fe_2O_5$ ($n = 2$), and the Grenier phase, $La_{0.33}Ca_{0.67}FeO_{2.67}$ ($n = 3$) [9–11].

The formation of a homogeneous solid solution in this system up to $x = 0.5$ was suggested in [12, 13]. For example, the authors of [13] concluded on the basis of X-ray analysis, redox titration, and temperature-programmed reduction (TPR) that, in the system synthesized by the citrate procedure, the homogeneous solid solutions are formed up to $x = 0.5$; they found an increase in the concentration of Fe^{4+} cations with an increase in the calcium concentration. Note that the authors found that the catalytic activity in the complete oxidation of methane did not depend on the concentration of Fe^{4+} cations in the samples.

In our studies [14–18] of this system prepared by ceramic and mechanochemical procedures, we did not observe the formation of a homogeneous solid solution over a wide range of x values (up to $x = 0.17$) but did find variations in the microstructure and phase composition of the samples prepared by different procedures. We found that three phases of the homologous series ($LaFeO_3$, $Ca_2Fe_2O_5$, and $La_{0.33}Ca_{0.67}FeO_{2.67}$) are formed in the samples of the ceramic series and only two

phases ($LaFeO_3$ and $Ca_2Fe_2O_5$) are formed in the samples of the mechanochemical series. Depending on the sample composition, these phases form microheterogeneous solid solutions with various microstructures. The Fe^{4+} cations were not found in the samples by Mössbauer spectroscopy [18]. At the same time, the catalytic activity in CO oxidation was found to depend on the sample composition and the samples with average compositions with a high density of phase boundaries exhibit the maximal activity. The facts that the phase boundaries are present in this system and their density is maximal in the region of average compositions and that the catalytic activity changes with a change in the density of the phase boundaries allowed us to suggest that additional coordinatively unsaturated sites can be formed at the phase boundaries on the surface. These sites are capable of adsorbing oxygen with the lowest bonding strength, which determines the enhanced activity of the samples of intermediate compositions.

Hence, various oxygen states can exist on the surface of perovskites in our system: oxygen located in the region of phase boundaries and on vacancies as well as lattice oxygen. TPR is one of the techniques that allows one to distinguish oxygen states.

Therefore, the goal of this work was to study oxygen states in the perovskite oxides $La_{1-x}Ca_xFeO_{3-y}$ prepared by different methods and to clarify the role of the surface and lattice oxygen states in the catalytic activity of perovskites of this series in the complete oxidation of CO and CH_4.

EXPERIMENTAL

The samples $La_{1-x}Ca_xFeO_{3-y}$ ($x = 0$, 0.2, 0.4, 0.6, 0.8, and 1.0) were prepared by the calcination of previously mechanically activated mixture of the initial oxides taken in the necessary ratios at 900 or 1100°C for 4 h. The duration of mechanical treatment was varied from 3 to 10 min, and the procedure of mechanochemical synthesis was described in [16]. The samples of the ceramic series were prepared by calcination of the initial oxides at 1100°C for 150 h; the ceramic synthesis was described in [17].

The catalytic activity in CO oxidation was studied at 300–500°C in a flow-circulation reactor with GC analysis of the reaction products. The fractions of the catalysts of 0.5–1 and 1–2 mm were used, and the sample weight was 1 g. The circulation rate was 1200 l/h, and the feed rate of the reaction mixture (1% CO + 1% O_2 in He) was 10 l/h. The specific catalytic activity was determined as the specific reaction rate at a CO concentration of 1% and calculated according to the formula

$$w, [\text{molecule CO m}^{-2} \text{ s}^{-1}]$$
$$= X/(1-X)(7.47 \times 10^{17}/S_{sp}), \quad (1)$$

where X is the CO conversion. The concentrations of components in the gaseous mixture were determined by chromatography with a maximal error of 20%.

The catalytic activity in CH_4 oxidation was studied at 350–600°C in a flow reactor with GC analysis of the reaction products. The fractions of the catalysts of 0.5–1 mm were used, and the sample weight was 1 g; the volume of the catalyst was 0.6 cm³. The feed rate of the reaction mixture (0.5% CH_4 + 9% O_2 in He) was 2.4 l/h (4000 h⁻¹). The reaction rate was calculated according to the formula

$$w, [\text{molecule CH}_4 \text{ m}^{-2} \text{ s}^{-1}] = kC_0 \times 2.69 \times 10^{19}, \quad (2)$$

where k, the effective first order rate constant, was calculated according to equation $k = -2.3 \log(1-X)/(tmS_{sp})$ for the plug-flow reactor (X is the CH_4 conversion, m is the sample weight, t is the contact time, $C_0 = 0.5$ is the initial CH_4 concentration, %). The error of chromatographic determination of the components in the gaseous mixture was at most 20%.

The samples (fraction 0.25–0.5 mm) were studied by temperature-programmed reduction with hydrogen in a flow setup with a thermal conductivity detector. Before reduction, the samples were treated with O_2 for 0.5 h at 500°C and cooled to room temperature in O_2. The weight of the sample was 50 mg, and the feed rate of the reductive mixture (10% H_2 in Ar) was 40 cm³/min. The samples were heated at a ramp of 10 K/min up to 900°C. The concentrations of the mixture components were estimated with an error of at most 20%. The peak areas under the TPR curves for the samples, which correspond to the hydrogen uptake (mmol/g of sample), were calculated using the profile of the asymmetric Gaussian function.

RESULTS AND DISCUSSION

Catalytic Properties of Substituted Perovskites $La_{1-x}Ca_xFeO_{3-y}$ in the Complete Oxidation Reactions

The catalytic activities of perovskites $La_{1-x}Ca_xFeO_{3-y}$ of the ceramic and mechanochemical series in carbon monoxide oxidation reach a maximum at average x values ($x = 0.4$–0.6). The data obtained are presented in Fig. 1.

The samples of the mechanochemical series prepared by 3-min mechanochemical treatment of the initial oxides followed by calcination at 1100°C for 4 h were tested in the catalytic reaction of the complete oxidation of methane (350–600°C) (Fig. 2). The selectivity to CO_2 was 100% irrespective of the temperatures of the tests and the composition of the samples. The close specific catalytic activities were found for nearly all the samples at these temperatures, and this finding coincides with the results reported in [13]. The only exception is the sample with the average composition ($x = 0.5$), and its activity was 2.5–4 times higher (depending on the temperature) than that of other samples (Fig. 2).
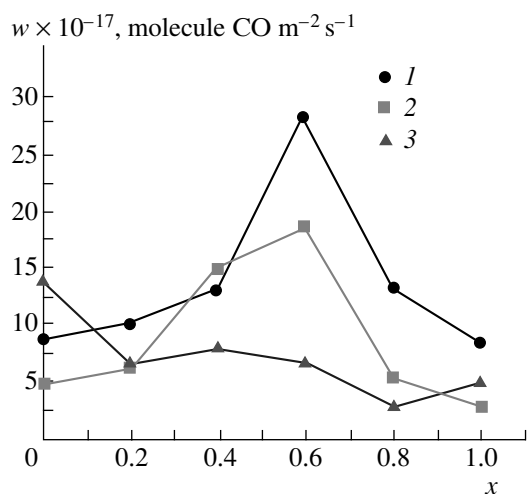
$w \times 10^{-17}$, molecule CO m^{-2} s^{-1}

Fig. 1. Specific reaction rate of CO oxidation at 450°C vs. the composition of samples La$_{1-x}$Ca$_x$FeO$_{3-y}$ (x) of the (*1*) ceramic and (*2, 3*) mechanochemical series after pretreatments: (*1*) calcination at 1100°C, 150 h; (*2*) 6 min of mechanochemical treatment, 1100°C, 4 h; (*3*) 6 min of mechanochemical treatment, 900°C, 4 h.

$w \times 10^{-16}$, molecule CH$_4$ m^{-2} s^{-1}

Fig. 2. Specific reaction rate of methane oxidation vs. the Ca concentration (x) in perovskite La$_{1-x}$Ca$_x$FeO$_{3-y}$ of the mechanochemical series (3 min of mechanochemical treatment, 1100°C, 4 h).

Hence, the sample with the intermediate composition in the series of substituted perovskites is the most active in catalytic oxidation of CH$_4$ as well as CO.

Based on earlier studies of the physicochemical properties of the perovskites of the above series, we found a correlation between a change in the specific catalytic activity upon the calcium introduction and the density of the phase boundaries determined by small-angle X-ray scattering (SAXS) as the integral intensity of X-ray scattering on microheterogeneities, including the regions of phase boundaries. The above density is maximal in the samples with intermediate compositions [16]. It was suggested that the active sites, the coordinatively unsaturated Fe^{3+} cations or clustered Fe^{2+} cations, can be formed at these phase boundaries on the surface. These sites are capable of adsorbing oxygen with low bonding strength, which is the most reactive species in complete oxidation [17]. TPR data for the samples prepared by different methods (Fig. 3) were analyzed from this point of view, and various oxygen states were found, as well as an increase in the concentration of weakly bound surface oxygen states in the samples with average compositions. TPR data for the samples are presented below.

Temperature-Programmed Reduction
of the Samples La$_{1-x}$Ca$_x$FeO$_{3-y}$

As follows from the data obtained (Fig. 3, table), an increase in the calcium content of the samples enhances their reducibility. Lanthanum ferrite begins to be reduced in the bulk at temperatures up to ~900°C irrespectively of the preparation conditions, whereas the bulk reduction of calcium ferrite from Fe^{3+} to Fe^0 is more than 80% completed by 900°C. Hence, the total
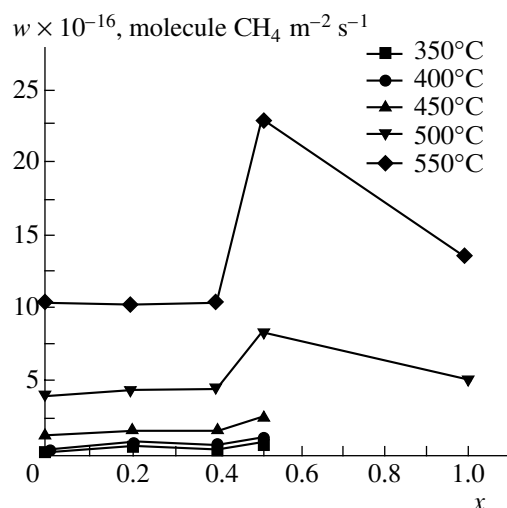
amount of oxygen removable during TPR changes in parallel with the calcium concentration (x) in the samples independently of the preparation conditions (Fig. 4, table).

Note that the samples are reduced in a wide temperature range. The TPR peaks have a complex shape and are split. This can be due to a diverse lattice and adsorbed oxygen states in perovskites and to the multiphase composition of the samples of each series. Three main regions of hydrogen uptake during the TPR of the samples can be identified.

(1) Low-temperature (<200°C) hydrogen uptake, which quantitatively corresponds to the removal of less than a monolayer of oxygen. Because oxide phases are not reduced in this temperature range, hydrogen uptake can characterize the most weakly bound surface oxygen states, including those adsorbed at extended defects on the surface.

(2) Hydrogen uptake in the temperature range 200–420°C, which is substantially lower than the reduction temperature for iron oxide α-Fe$_2$O$_3$. The amount of removable oxygen (from one to several tens of monolayers) points to the subsurface reduction of perovskites. In this temperature range, oxygen bound to vacancies in the subsurface oxide layers is removed, because this system belongs to vacancy perovskites. Oxygen incorporated in the interphase boundaries are removed as well, as the maximal amount of such oxygen is found for samples with the intermediate composition.

(3) Uptake in the range of moderate (450–700°C) and high (≥700°C) temperatures quantitatively corresponds to deeper reduction of oxides (see table) and therefore can be ascribed to the bulk reduction of per-
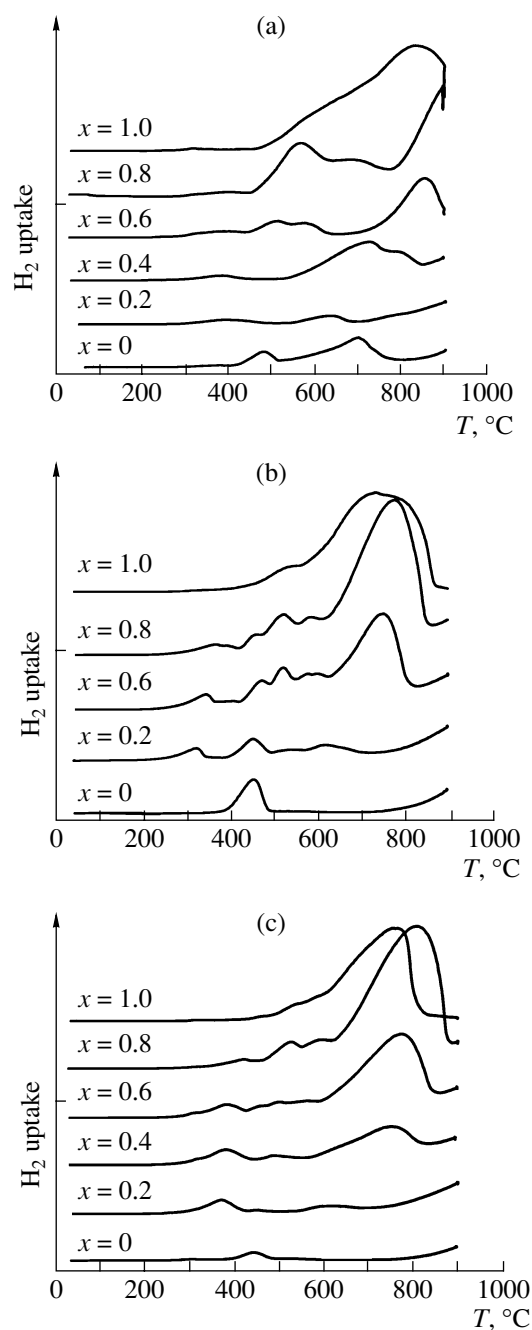
Fig. 3. TPR curves for perovskite $La_{1-x}Ca_xFeO_{3-y}$: (a) ceramic series (1100°C, 150 h); (b) mechanochemical series (6 min of mechanochemical treatment, 900°C, 4 h); and (c) mechanochemical series (6 min of mechanochemical treatment, 1100°C, 4 h).

Fig. 4. Total hydrogen uptake and hydrogen uptake in the range (a) below 400, (b) 420, and (c) 425°C vs. the composition of samples (x): (a) ceramic series (1100°C, 150 h); (b) mechanochemical series (6 min of mechanochemical treatment, 1100°C, 4 h); and (c) mechanochemical series (6 min of mechanochemical treatment, 900°C, 4 h).

ovskites, for example, the reduction of Fe^{3+} to Fe^{2+} and further to Fe^0 in the perovskite structure.

Let us consider the TPR data in more detail and compare them with data on the catalytic activity taking into account the above division into groups.

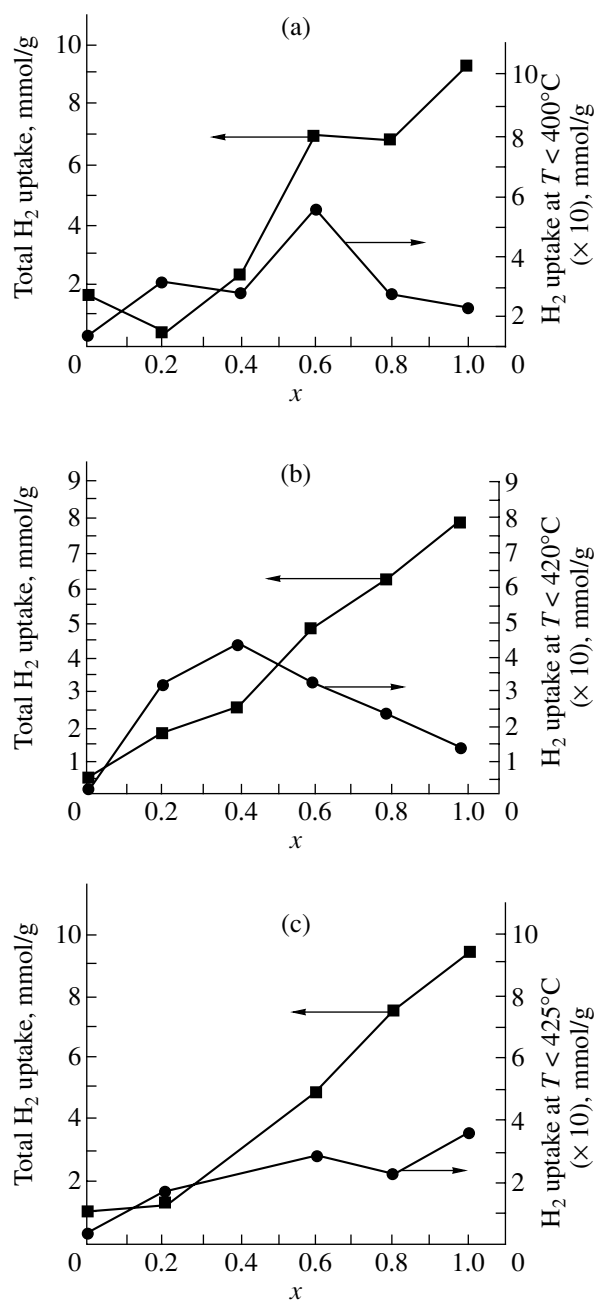The dependence of the amount of hydrogen consumed at temperatures below 200°C (when nearly a monolayer of oxygen is removed) on the sample composition has an extremum. The maximal amount of consumed hydrogen was found for the samples with average compositions (see the data in table for samples calcined at 1100°C), and their catalytic activity changes with the composition in a similar way. Moreover, as follows from Fig. 5, one can construct with higher or

TPR of perovskites $La_{1-x}Ca_xFeO_{3-y}$

x	Total H$_2$ uptake, mmol/g	Hydrogen uptake, mmol/g in temperature range of					
		up to 200°C	350–400°C	450–480°C	510–590°C	620–730°C	890–1150°C
Ceramic series (1100°C, 150 h)							
0	1.70	0.043	0.042 (350)	0.310 (480)	–	1.300 (700)	–
0.2	0.49	0.066	0.216 (400)	–	–	0.275 (635)	–
0.4	2.36	0.0623	0.176 (380)	–	–	1.820 (730)	0.540 (790)
0.6	6.94	0.1211	0.457 (400)	–	0.943 (516) 0.771 (575)	–	4.770 (860)
0.8	6.84	0.0463	0.176 (370)	–	2.20 (540)	1.260 (650)	3.200(*)
1.0	9.26	0.01467	0.130 (320)	–	–	–	9.130 (840)
Mechanochemical series (6 min of mechanical treatment, 1100°C, 4 h)							
0	0.59	0.0032	0.026 (310)	0.174 (450)	0.050 (540)	–	0.340 (*)
0.2	1.83	0.004	0.324 (370)	0.062 (450)	–	0.326 (620)	1.120 (*)
0.4	2.59	0.0583	0.058 (320) 0.380 (385)	0.240 (490)	–	0.280 (640)	1.640 (755)
0.6	4.84	0.147	0.052 (320) 0.280 (385)	0.148 (465)	0.178 (500)	0.280 (680)	3.900 (755)
0.8	8.30	0.09	0.240 (420)	–	0.500 (520) 0.460 (574)	–	6.840 (810) 0.260 (900)
1.0	–	0.0836	–	–	–	–	–
Mechanochemical series (6 min of mechanical treatment, 900°C, 4 h)							
0	1.05	0.013	0.007 (360)	0.509 (460)	0.060 (540)	–	0.472 (*)
0.2	1.25	0.003	0.231 (330)	0.346 (460)	0.192 (550)	0.481 (620)	–
0.6	4.90	0.0094	0.269 (350) 0.077 (410)	0.365 (477)	0.500 (530) 0.635 (580)	–	3.060 (755)
0.8	7.51	0.126	0.181 (370) 0.085 (400)	0.171 (465)	0.692 (530) 0.461 (590)	–	5.920 (780)
1.0	9.39	0.208	–	0.206 (450)	0.697 (540)	–	8.48 (740–780)

Note: Temperatures (°C) of the peak maxima are presented in parentheses.

    * Peak is above 900°C, i.e., is beyond the limits of measurement.

lower accuracy (with a correlation coefficient of 0.67–0.96) linear relationships between the amount of oxygen removed from the unit of the surface area of the samples and their specific (related to 1 m^2) catalytic activity for each of the series studied. Note that a correlation exists between the concentration of oxygen states and the specific catalytic activity for samples with the same composition prepared by different methods. An increase in the temperature or duration of sintering results in an increase in the surface coverage with weakly bound oxygen states and the specific catalytic activity. The results obtained point to the relation between the specific catalytic activity of perovskites and the amount of this oxygen state and also suggest that this oxygen can be located at phase boundaries on the surface.

The peaks in the temperature range 350–470°C can be divided into two groups: peaks with maxima in the 350–420 and 450–470°C ranges, respectively. It is of interest that the hydrogen uptakes in these two regions change in a different way with the composition of the samples of all series. The peak at 470°C decreases with an increase in x, whereas the uptake in the 350–400°C range passes through a maximum for the intermediate

compositions in all the series studied (Fig. 4). As the uptake in the 450–470°C range is most typical of lanthanum ferrite (Fig. 3) and all the samples with intermediate x values are not single-phase, then a decrease in the uptake in this temperature range with increasing x can be ascribed to a decrease in the concentration of the lanthanum ferrite phase in the samples.

According to the reported data, small peaks of hydrogen uptake in the 450–480°C range typical of lanthanum ferrite were attributed to either the reduction of tetravalent iron cations (Fe^{4+} to Fe^{3+}) [12, 13] or the removal of overstoichiometric oxygen and/or the formation of $La_{0.9}FeO_{2.95}$, which is stable in a reductive atmosphere [19]. The estimated concentration of Fe^{4+} cations in the sample with $x = 0$ of the ceramic series is ~15% of the total concentration of iron cations. However, we failed to find Fe^{4+} cations by Mössbauer spectroscopy in the samples of the ceramic series [18]. Therefore, the presence of the peak for hydrogen uptake with a maximum at 450°C in the TPR spectrum of lanthanum ferrite of the ceramic series can be assigned to the partial oxygen removal and the formation of $La_{0.9}FeO_{2.95}$. Unlike the case reported in [13], the absence of Fe^{4+} cations in our samples could be due to different preparation conditions, since the citrate procedure for perovskite synthesis was used in [13].

A specific change in hydrogen uptake in the 350–420°C range as a function of the chemical composition of the sample, which is maximal for the samples with average compositions (Fig. 4), has not been reported previously. As follows from the above data, the uptake in this range cannot be due to the appearance of Fe^{4+} cations upon the calcium introduction. This uptake was not observed in the samples with $x = 1$ and 0, and this fact rules out its relation with any phase similar to the uptake in the 450–470°C range. The uptake in this temperature range changes in parallel with the variation in the density of the phase boundaries. Taking into account that the amount of hydrogen consumed in these peaks corresponds to the removal of one or several tens of oxygen monolayers, one can assume that the phase boundaries facilitate the reduction of either each phase or any one phase. In our opinion, this peak can be attributed to the reduction of the vacancy-ordered Grenier phase, which is not completely ordered inside microheterogeneous solutions [18] and is characterized, according to the Mössbauer spectroscopic data, by the presence of five-coordinated Fe^{3+} cations.

In the samples of the mechanochemical series, the positions of the consumption peaks H_2 and their intensities in the above temperature range of consumption change similarly. Therefore, the presence of at least two different species of adsorbed oxygen at 350–420°C can also be explained by the presence of phases of calcium ferrite and lanthanum ferrite in the samples with different degree of vacancy ordering in the vicinity of phase boundaries.
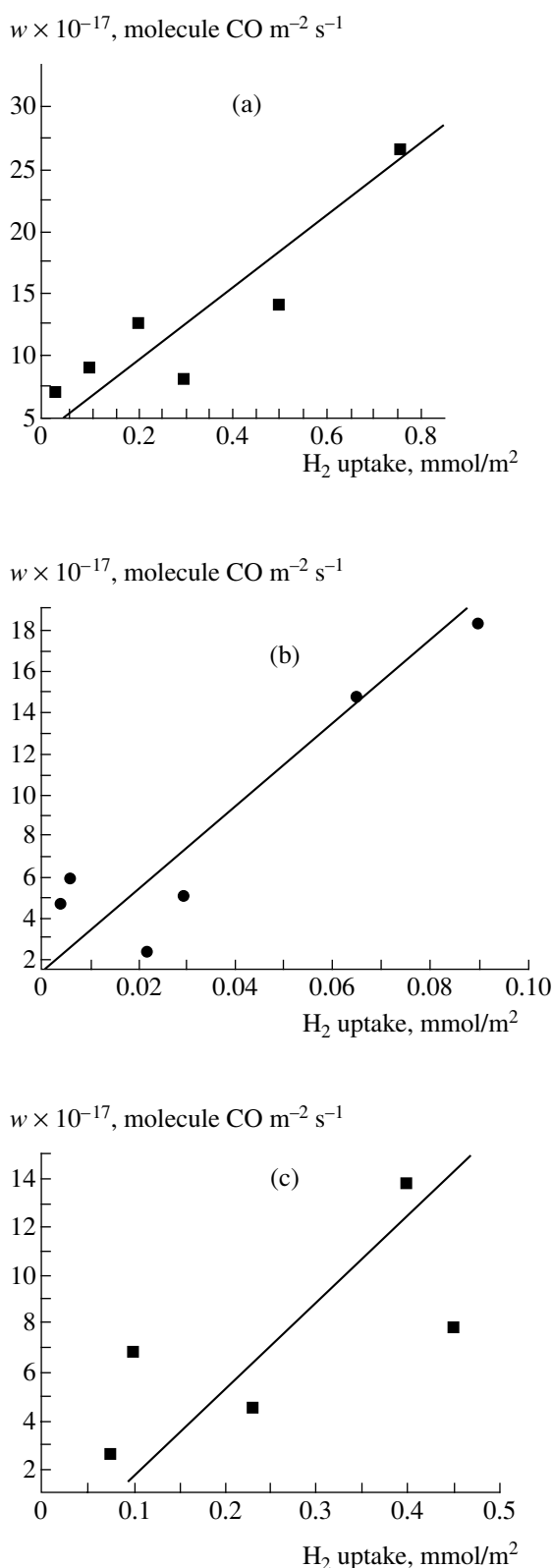
$w \times 10^{-17}$, molecule CO m^{-2} s^{-1}

$w \times 10^{-17}$, molecule CO m^{-2} s^{-1}

$w \times 10^{-17}$, molecule CO m^{-2} s^{-1}

Fig. 5. Specific reaction rate of CO oxidation at 450°C vs. the amount of consumed H_2 in the range below 200°C for samples of the (a) ceramic series (1100°C, 150 h); (b) mechanochemical series (6 min of mechanochemical treatment, 1100°C, 4 h); and (c) mechanochemical series (6 min of mechanochemical treatment, 900°C, 4 h).
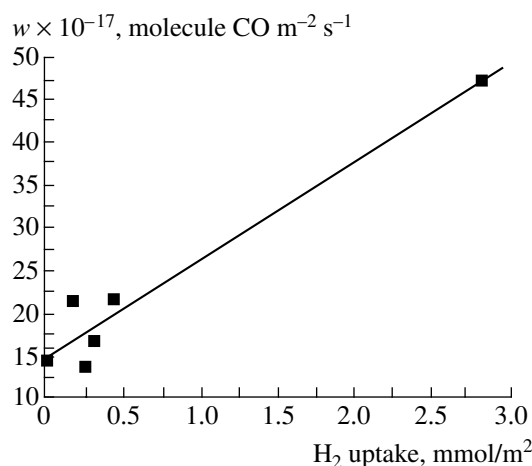
$w \times 10^{-17}$, molecule CO m^{-2} s^{-1}

Fig. 6. Specific reaction rate of CO oxidation at 500°C vs. the amount of consumed H$_2$ in the range below 400°C for samples of ceramic series.

Hence, the main feature of the TPR spectra in the low-temperature range in which the subsurface oxygen states is removed is a nonmonotonic change in the hydrogen uptake with the sample composition. The hydrogen uptake maxima are observed at the average compositions of the series under study, and this corresponds to a change in the specific catalytic activity (with a correlation coefficient of 0.92) in the complete oxidation reactions (Fig. 6).

In the range of moderate temperatures (470–730°C), one can additionally separate two groups of peaks on the TPR curves with maxima at 510–590°C and 635–730°C, depending on the preparation conditions and chemical composition. In these peaks, the amount of consumed hydrogen corresponds to the bulk reduction of Fe^{3+} to Fe^{2+} cations in the samples and this fact agrees with the data presented in [13]. When the calcium concentration increases, the amount of consumed hydrogen in this temperature range increases monotonically, possibly due to the better reducibility of both the Grenier phases and calcium ferrite (whose concentrations also increase) and the perovskite phase located in the proximity of the phase boundaries. Thus, even during the bulk reduction of the samples, the process cannot be described by the simple summing of the TPR curves for the constituent phases, and the effect of the phase boundaries on the phase reducibility manifests itself at the deeper reduction stages. We cannot rule out that in the temperature range 510–590°C, the admixed phases Fe_2O_3 and $CaFe_2O_4$ in the samples can be partially or completely reduced. Nevertheless, no dependence between the catalytic performance in complete oxidation and hydrogen uptake by the samples was found despite a variety of the reduction peaks in this temperature range.

The TPR curves in the temperature range above 800°C for all the series under study are characterized by a low-temperature shift of the maxima with increasing calcium content (*x*) and by an increase in the hydrogen uptake. Note that the reduction degrees, other conditions being equal, are higher for the samples of the mechanochemical series. The fact that the reducibility of the sample depends on the preparation procedure was confirmed by data presented in [20] where the reduction of iron cations of perovskite to metallic iron was found at 800–900°C. However, despite the deeper reduction of the samples (practically up to Fe^0) achieved in this work, no linear dependence between the specific catalytic activity and the total hydrogen uptake was observed.

The data presented here suggest that the strongly bound species of the perovskite lattice oxygen do not participate in the catalytic oxidation of both carbon monoxide and methane as is the case of simple oxides [7].

The found correlation between a change in the catalytic activity of the samples and their surface (up to 200°C) and subsurface (320–420°C) reduction does not contradict the conclusions of [1, 2, 4] on the stepwise mechanism of CO oxidation over perovskites. The existence of the reactive oxygen states on the surface is likely determined by the presence of the phase boundaries. Clusters of the coordinatively unsaturated Fe^{2+} cations can be formed at these boundaries on the surface. These clusters are capable of adsorbing the most weakly bound oxygen states [21]. Near these boundaries, the stage of the subsurface reduction of oxides is facilitated possibly due to the reduction of oxygen adsorbed on vacancies whose concentration, as is well known, is enhanced near the extended defects.

The fact that the specific catalytic activity is proportional to the concentration of the most weakly bound oxygen states for all the samples irrespectively of the composition or preparation conditions may also indicate a common nature for the catalytically active sites of the perovskites of the series under study. In [22], the occurrence of clusters of the coordinatively unsaturated reduced Fe^{2+} cations on the surface of lanthanum ferrite and calcium ferrite was found by IR spectroscopy of probe molecules. Based on these data, we can suggest that the same sites are the most active in all the samples under study.

The weaker dependence of the activity of samples on their composition in methane oxidation can be explained by either a lesser reduction degree of the surface in a methane-containing reaction medium compared to CO or by a higher coverage of the surface with water formed during the reaction. It is well known that hydroxylation of the surface decreases the concentration of the coordinatively unsaturated sites, iron cations in this case. Hence, the effects observed can be rationalized on the basis of the fact that the most active sites are blocked first.

REFERENCES

1. Seiyama, T., *Catal. Rev. – Sci. Eng.*, 1991, vol. 34, no. 4, p. 281.
2. Yamazoe, N. and Teraoka, V., *Catal. Today*, 1990, vol. 8, no. 2, p. 175.
3. Tejuca, L.G., Fierro, J.L.G., and Tascon, J.M.D., *Adv. Catal.*, 1989, vol. 36, p. 237.
4. Baran, E.J., *Catal. Today*, 1990, vol. 8, p. 133.
5. Popovskii, V.V., *Teoreticheskie problemy kataliza* (Theoretical Problems of Catalysis), Novosibirsk: Inst. of Catalysis, 1977, p. 81.
6. Boreskov, G.K., *Geterogennyi kataliz* (Heterogeneous Catalysis), Moscow: Nauka, 1988, p. 304.
7. Sadykov, V.A., Tikhov, S.F., Tsybulya, S.V., Kryukova, G.N., Veniaminov, S.A., Kolomiichuk, V.N., Bulgakov, N.N., Isupova, L.A., Paukshtis, E.A., Zaikovskii, V.I., Kustova, G.N., and Burgina, E.B., *Stud. Surf. Sci. Catal.*, 1997, vol. 110, p. 1155.
8. Li, R., Ma, J., Zhou, X., and Su, Zh., *React. Kinet. Catal. Lett.*, 2000, vol. 70, no. 2, p. 362.
9. Grenier, J.-C., Pouchard, M., and Hagenmuller, P., *Structure and Bonding*, Berlin: Springer, 1981, vol. 47.
10. Alario-Franco, M.A., Calbet, J.M.G., Regi, M.V., and Grenier, J.-C., *J. Solid State Chem.*, 1983, vol. 49, p. 219.
11. Grenier, J.-C., Fournes, L., Pochard, M., Hagenmuller, P., and Komornicky, S., *Mat. Res. Bull.*, 1982, vol. 17, p. 55.
12. Rao, C.N.R., Gopalakrishnan, J., and Vidyasagar, K., *Indian J. Chem., Sect. A*, 1984, vol. 23, p. 265.
13. Ciambelli, P., Cimino, S., Lisi, L., Faticanti, M., Minelli, G., Pettiti, I., and Prota, P., *Appl. Catal., B*, 2001, vol. 33, p. 193.
14. Isupova, L.A., Yakovleva, I.S., Tsybulya, S.V., Kryukova, G.N., Boldyreva, N.N., Alikina, G.M., Vlasov, A.A., Ivanov, V.P., and Sadykov, V.A., *Kinet. Katal.*, 2000, vol. 41, no. 2, p. 315.
15. Isupova, L.A. and Tsybulya, S.V., *Book of Absracts of ECSSSC'99*, Madrid, 1999, vol. 1, p. O4.
16. Isupova, L.A., Tsybulya, S.V., Kryukova, G.N., Alikina, G.M., Boldyreva, N.N., Vlasov, A.A., Snegurenko, O.I., Ivanov, V.P., Kolomiichuk, V.N., and Sadykov, V.A., *Kinet. Katal.*, 2002, vol. 43, no. 1, p. 140.
17. Isupova, L.A., Yakovleva, I.S., Tsybulya, S.V., Kryukova, G.N., Boldyreva, N.N., Alikina, G.M., Rogov, V.A., Vlasov, A.A., and Sadykov, V.A., *Khim. Interes. Ust. Razv.*, 2002, no. 10, p. 77.
18. Isupova, L.A., Yakovleva, I.S., Gainutdinov, I.I., Pavlyikhin, Yu.T., and Sadykov, V.A., *React. Kinet. Catal. Lett.*, 2004, vol. 81, no. 2.
19. Belessi, V.C., Trikalitis, P.N., Labados, A.K., Bakas, T.V., and Povonis, P.J., *Appl. Catal., A*, 1999, vol. 177, p. 53.
20. Zhong, Z., Chen, K., Yi, Y., and Yan, Q., *Appl. Catal., A*, 1997, vol. 156, p. 29.
21. Bulgakov, N.N. and Sadykov, V.A., *React. Kinet. Catal. Lett.*, 1996, vol. 58, no. 2, p. 397.
22. Isupova, L.A., Budneva, A.A., Paukshtis, E.A., and Sadykov, V.A., *J. Mol. Catal. A: Chem.*, 2000, vol. 158, p. 275.